Article

Conical-Shaped Shells of Non-Uniform Thickness Vibration Analysis Using Higher-Order Shear Deformation Theory

Saira Javed

Department of Mathematics and Statistics, College of Science, King Faisal University, P.O. Box 400, Al Ahsa 31982, Saudi Arabia; sulhaque@kfu.edu.sa

Abstract: The aim of this research is to investigate the frequency of conical-shaped shells, consisting of different materials, based on higher-order shear deformation theory (HSDT). The shells are of non-uniform thickness, consisting of two to six symmetric cross-ply layers. Simply supported boundary conditions were used to analyse the frequency of conical-shaped shells. The differential equations, consisting of displacement and rotational functions, were approximated using spline approximation. A generalised eigenvalue problem was obtained and solved numerically for an eigenfrequency parameter and associated eigenvector of spline coefficients. The frequency of shells was analysed by varying the geometric parameters such as length of shell, cone angle, node number in circumference direction and number of layers, as well as three thickness variations such as linear, sinusoidal and exponential. It was also evident that by varying geometrical parameters, the mechanical parameters such as stress, moment and shear resultants were affected. Research results concluded that for three different thickness variations, as the number of layers of conical shells increases, the frequency values decrease. Moreover, by varying length ratios and cone angles, shells with variable thickness had lower frequency values compared to shells of constant thickness. The numerical results obtained were verified through the already existing literature. It is evident that the present results are very close to the already existing literature.

Keywords: analysis; vibration; variable thickness; eigenfrequency; higher-order theory

1. Introduction

Composite shells have been widely used in marine, mechanical and aeronautical engineering. Conical shells are used in numerous structures, e.g., in submarine and offshore structures, aircraft, tubular structures, towers and tanks. Conical shells of variable thickness can be used in various engineering applications, such as pressure vessels, storage tanks and aerospace structures. The variable thickness allows for optimisation of the shell's weight and strength, making it a versatile design choice. Additionally, the conical shape provides structural stability and efficient load distribution. Overall, the use of conical shells of variable thickness can offer a balance between performance and material efficiency in engineering designs. Properties such as high stiffness to weight and low density are striking features of composites, which are particularly useful for engineering structures because they require high stiffness and light weight. Shells are considerably stronger and stiffer than other structural forms, since they efficiently resist applied external loads by virtue of their geometrical form, i.e., spatial curvatures. Owing to this, the present study is based on conical shell structures. Conical shells of non-uniform thickness have better stress and strain distributions, as well as an optimum weight compared to shells of uniform thickness, and it is important to know how the mechanical properties, such as natural frequency, are influenced by varying the dimensions and geometrical parameters of the shell. Composite structures of variable thickness are used in many engineering fields. Moreover, conical shells of variable thickness have been vastly used in the aerospace and missile industries. The purpose of variable thickness is to obtain a required stable structure or to acquire a

required frequency. There are a number of theories that accurately predict the structural and dynamic behaviour of composite structures. Among them, composite plates and shells can be analysed with reasonable accuracy using the equivalent single-layer [1,2] and layer-wise [3] theories based on the 2D descriptions of the structures. In the equivalent single-layer theories, mid-plane displacements are considered as field variables and are described through the thickness variation of displacements over the assumed deformation of the cross-section. The equivalent single-layer formulations are usually simpler compared to layer-wise formulations and are easier to apply in numerical procedures, providing accurate displacement and stress components, particularly for thin and moderately thick laminates. Free vibration analysis of rotating functionally graded conical shells were examined and investigated [4]. The higher-order shear deformation theory, used to analyse the free vibration of stiffened rotating FGM conical shells in a thermal environment, was studied [5]. Moreover, the nonlinear free vibration analysis of truncated conical shells, made of bidirectional functionally graded materials, was examined [6]. Ref. [7] investigated the modeling and free vibration analysis of variable stiffness systems for sandwich conical shell structures with variable thickness. Functionally graded CNT-reinforced composite conical shell panels were studied [8]. The Chebyshev-RPIM meshless solution for the free vibration of conical shell panels with variable thickness and fiber curvature was examined by [9]. Free vibration analyses of rotating cross-ply laminated combined elliptical–cylindrical–conical shells have also been investigated [10]. Zigzag theories [11] are combinations of the equivalent single-layer and layer-wise theories. Zigzag theories are as computationally efficient as single-layer theories and can produce as accurate predictions as layer-wise theories. Moreover, higher-order shear deformation theory calculates more precise inter-laminar stress distributions and satisfies the conditions of zero-shear stress at the top and bottom surfaces of the plate. In addition, in higher-order theory, the displacement component is expanded up to the third power term along z-coordinates, in order to have a fourth power variation of transverse shear strains and transverse shear stresses through the plate thickness (Reddy [12]). The free vibration of conical shells using HSDT in thermal surrounding were examined by Singha et al. [13]. Deb Singha et al. [14] analysed pre-twisted conical shells with functionally graded carbon nanotube. The frequencies of coupled conical shells have also been investigated (Gia Ninh [15] and Bagheri [16]). The DQM method was used to study conical and cylindrical shells and annular circular plates by Safarpour et al. [17]. GNP-reinforced conical shells were investigated by Afshari [18]. Refined shear deformation theory has been used to analyse the nonlinear forced vibration of conical shells (Amabili and Balasubramanian [19]). Using HSDT and DQM, the buckling and vibration of annular plates were analysed by Zhang et al. [20]. Taati et al. [21] investigated the free vibration of cylindrical shells of variable thickness using a closed form solution. Sandwich conical shells were studied by Zarei et al. [22]. The Walsh series technique was used by Guo et al. [23] to examine the frequencies of cone-shaped shells. Maji and Singh [24] used shear deformation theory to investigate the free vibration of conical shells under rotation. The Haar wavelet technique was used to analyse functionally graded conical shells in order to study free vibration and buckling behaviours by Pakravan et al. [25]. Immersed cylinder-shaped shells of varying thickness were studied by Wang et al. [26]. Functionally graded plates were analysed by Thai et al. [27]. Phung-Van et al. [28] examined multilayer functionally graded graphene platelet-reinforced composite nanoplates. This current study is different in one way or another when compared with all of the above-mentioned studies. None of the studies used the spline approximation method, nor composite materials consisting of six layers, each of different materials.

This research work aims to investigate the frequency of conical-shaped shells consisting of different materials based on higher-order shear deformation theory (HSDT). The shells are of non-uniform thickness, consisting of two to six symmetric cross-ply layers. The advantage of the proposed solution methodology is to obtain lower, desired frequency values, and to achieve structural stability, as well as to reduce the weight, size and cost of construction. The novelty of this present work is that it examines the free vibration

of conical-shaped shells of variable thickness consisting of two to six layers under the influence of higher-order shear deformation theory for simply supported end conditions using the spline approximation method. Moreover, the frequencies of constant and variable thickness shells are compared. The frequencies of shells, by varying the geometric parameters such as length of shell, cone angle, node number in circumference direction and number of layers, as well as three thickness variations such as linear, sinusoidal and exponential, are examined. It is also evident that by varying the geometrical parameters, the mechanical parameters, such as stress, moment and shear resultants, are affected. Graphs and tables depict the obtained results.

The main motivation of this study is to investigate the vibration of shells and to achieve lower frequency values for more stable structures. In order to achieve this aim, shells of non-uniform thickness and consisting of different layers were considered. Generally, for shell structures, lower frequencies are often preferred as they indicate larger, more global modes of vibration that are typically easier to control and dampen. It is evident from the obtained results that as the number of layers of conical shells increases, the frequency values decrease. Moreover, by varying length ratios and cone angles, shells with non-uniform thickness have lower frequency values compared to shells of constant thickness. So, our objective to achieve lower frequency values was fulfilled by non-uniform thickness and increasing the number of layers of shell.

2. Solution of Problem

The displacement fields considered are based on third-order shear deformation theory (Reddy [12]). Two different shear deformation theories are visualised in Figure 1.

First shear deformation theory

Higher shear deformation theory
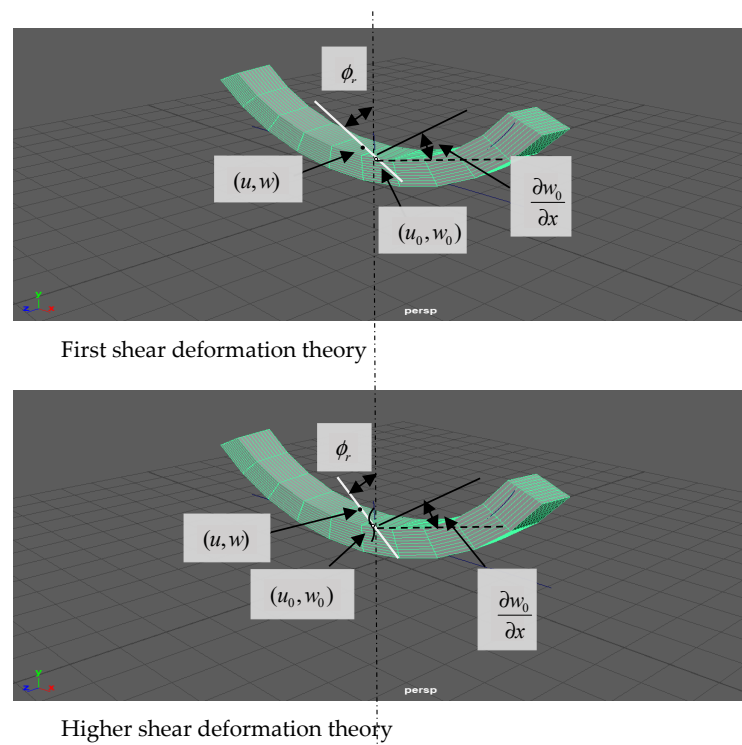
Figure 1. Deformation theories.

A laminated conical shell of variable thickness along the axial direction, having an arbitrary number of layers that are perfectly bonded together, is shown in Figure 2. The orthogonal coordinate system (x, θ, z) is fixed at its reference surface, which is taken to be at the middle surface. The radius of the cone at any point along its length is $r = x \sin \alpha$. The radius at the small end of the cone is $r_a = a \sin \alpha$ and the other end is $r_b = b \sin \alpha$. α is the semi-vertical angle and ℓ is the length of the cone along its generator.

The displacement field was considered according to third-order shear deformation theory by Reddy [12].

$$
\begin{aligned}
u(x,y,z,t) &= u_0(x,y,t) + z\phi_x(x,y,t) - \frac{4z^3}{3h^2}\left(\phi_x + \frac{\partial w_0}{\partial x}\right) \\
v(x,y,z,t) &= v_0(x,y,t) + z\phi_\theta(x,y,t) - \frac{4z^3}{3h^2}\left(\phi_\theta + \frac{\partial w_0}{\partial y}\right) \\
w(x,y,z,t) &= w_0(x,y,t)
\end{aligned}
\tag{1}
$$

where u, v and w are the displacement components in the x, θ and z directions, respectively, u_0, v_0 and w_0 are the in-plane displacements of the middle plane, and ϕ_x and ϕ_θ are the shear rotations at any point on the middle surface of the plate.

The stress resultants are defined (Reddy [12]) as follows:

$$
\begin{Bmatrix} N_r \\ N_\theta \\ N_{r\theta} \end{Bmatrix} = \int_{-h/2}^{h/2} \begin{Bmatrix} \sigma_r \\ \sigma_\theta \\ \sigma_{r\theta} \end{Bmatrix} dz, \quad
\begin{Bmatrix} M_r \\ M_\theta \\ M_{r\theta} \end{Bmatrix} = \int_{-h/2}^{h/2} z \begin{Bmatrix} \sigma_r \\ \sigma_\theta \\ \sigma_{r\theta} \end{Bmatrix} dz, \quad
\begin{Bmatrix} O_r \\ O_\theta \\ O_{r\theta} \end{Bmatrix} = \int_{-h/2}^{h/2} z^3 \begin{Bmatrix} \sigma_r \\ \sigma_\theta \\ \sigma_{r\theta} \end{Bmatrix} dz
$$

$$
\begin{Bmatrix} Q_\theta \\ Q_r \end{Bmatrix} = \int_{-h/2}^{h/2} z^2 \begin{Bmatrix} \tau_{\theta z} \\ \tau_{rz} \end{Bmatrix} dz \text{ and } \begin{Bmatrix} R_\theta \\ R_r \end{Bmatrix} = \int_{-h/2}^{h/2} z^2 \begin{Bmatrix} \tau_{\theta z} \\ \tau_{rz} \end{Bmatrix} dz
\tag{2}
$$

where N, M and Q are stress, moment and shear resultants, respectively. Higher stress resultants are O and R.

The stress–strain relations (Reddy [12]) were obtained as follows:

$$
\begin{Bmatrix} N_r \\ N_\theta \\ N_{r\theta} \\ M_r \\ M_\theta \\ M_{r\theta} \\ O_r \\ O_\theta \\ O_{r\theta} \end{Bmatrix} =
\begin{pmatrix}
A_{11} & A_{12} & A_{16} & B_{11} & B_{12} & B_{16} & E_{11} & E_{12} & E_{16} \\
A_{12} & A_{22} & A_{26} & B_{12} & B_{22} & B_{26} & E_{12} & E_{22} & E_{26} \\
A_{16} & A_{26} & A_{66} & B_{16} & B_{26} & B_{66} & E_{16} & E_{26} & E_{66} \\
B_{11} & B_{12} & B_{16} & D_{11} & D_{12} & D_{16} & F_{11} & F_{12} & F_{16} \\
B_{12} & B_{22} & B_{26} & D_{12} & D_{22} & D_{26} & F_{12} & F_{22} & F_{26} \\
B_{16} & B_{26} & B_{66} & D_{16} & D_{26} & D_{66} & F_{16} & F_{26} & F_{66} \\
E_{11} & E_{12} & E_{16} & F_{11} & F_{12} & F_{16} & H_{11} & H_{12} & H_{16} \\
E_{12} & E_{22} & E_{26} & F_{12} & F_{22} & F_{26} & H_{12} & H_{22} & H_{26} \\
E_{16} & E_{26} & E_{66} & F_{16} & F_{26} & F_{66} & H_{16} & H_{26} & H_{66}
\end{pmatrix}
\begin{Bmatrix}
\varepsilon_r^{(0)} \\ \varepsilon_\theta^{(0)} \\ \gamma_{r\theta}^{(0)} \\ \varepsilon_r^{(1)} \\ \varepsilon_\theta^{(1)} \\ \gamma_{r\theta}^{(1)} \\ \varepsilon_r^{(3)} \\ \varepsilon_\theta^{(3)} \\ \gamma_{r\theta}^{(3)}
\end{Bmatrix},
\tag{3}
$$

$$
\begin{Bmatrix} Q_\theta \\ Q_r \\ R_\theta \\ R_r \end{Bmatrix} =
\begin{pmatrix}
A_{44} & A_{45} & D_{44} & D_{45} \\
A_{45} & A_{55} & D_{45} & D_{55} \\
D_{44} & D_{45} & F_{44} & F_{45} \\
D_{45} & D_{55} & F_{45} & F_{55}
\end{pmatrix}
\begin{Bmatrix}
\gamma_{\theta z}^{(0)} \\ \gamma_{rz}^{(0)} \\ \gamma_{\theta z}^{(2)} \\ \gamma_{rz}^{(2)}
\end{Bmatrix}
$$

where ε is strain and γ is the shear strain components. Details regarding A_{ij}, B_{ij}, D_{ij}, E_{ij}, F_{ij}, H_{ij}, can be found in Ref. [29].

In-plane strains are defined as

$$
\varepsilon = \begin{Bmatrix} \varepsilon_x \\ \varepsilon_\theta \\ \gamma_{x\theta} \end{Bmatrix}
$$

$$
\varepsilon = \varepsilon^0 + z\varepsilon^1 + z^3\varepsilon^3 = \begin{Bmatrix} \varepsilon_x^0 \\ \varepsilon_\theta^0 \\ \gamma_{x\theta}^0 \end{Bmatrix} + z\begin{Bmatrix} \varepsilon_x^1 \\ \varepsilon_\theta^1 \\ \gamma_{x\theta}^1 \end{Bmatrix} + z^3\begin{Bmatrix} \varepsilon_x^3 \\ \varepsilon_\theta^3 \\ \gamma_{x\theta}^3 \end{Bmatrix}
\tag{4}
$$

and the shear strain components are defined as

$$
\gamma = \left\{ \begin{array}{c} \gamma_{\theta z} \\ \gamma_{xz} \end{array} \right\}
$$
$$
\gamma = \gamma^0 + z^2 \gamma^2 = \left\{ \begin{array}{c} \gamma_{\theta z}^0 \\ \gamma_{xz}^0 \end{array} \right\} + z^2 \left\{ \begin{array}{c} \gamma_{\theta z}^2 \\ \gamma_{xz}^2 \end{array} \right\}
$$
(5)

When the materials are oriented at an angle θ with the x-axis, the transformed stress–strain relations are

$$
\left(\begin{array}{c} \sigma_x^{(k)} \\ \sigma_\theta^{(k)} \\ \tau_{x\theta}^{(k)} \\ \tau_{\theta z}^{(k)} \\ \tau_{xz}^{(k)} \end{array} \right) = \left(\begin{array}{ccccc} \overline{Q}_{11}^{(k)} & \overline{Q}_{12}^{(k)} & \overline{Q}_{16}^{(k)} & 0 & 0 \\ \overline{Q}_{12}^{(k)} & \overline{Q}_{22}^{(k)} & \overline{Q}_{26}^{(k)} & 0 & 0 \\ \overline{Q}_{16}^{(k)} & \overline{Q}_{26}^{(k)} & \overline{Q}_{66}^{(k)} & 0 & 0 \\ 0 & 0 & 0 & \overline{Q}_{44}^{(k)} & \overline{Q}_{45}^{(k)} \\ 0 & 0 & 0 & \overline{Q}_{45}^{(k)} & \overline{Q}_{55}^{(k)} \end{array} \right) \left(\begin{array}{c} \varepsilon_x^{(k)} \\ \varepsilon_\theta^{(k)} \\ \gamma_{x\theta}^{(k)} \\ \gamma_{\theta z}^{(k)} \\ \gamma_{xz}\gamma_{xz}^{(k)} \end{array} \right)
$$
(6)

where $\overline{Q}_{ij}^{(k)}$ is defined as follows

$$
\overline{Q}_{11}^{(k)} = Q_{11}^{(k)}\cos^4\theta + Q_{22}^{(k)}\sin^4\theta + 2\left(Q_{12}^{(k)} + 2Q_{66}^{(k)}\right)\sin^2\theta\cos^2\theta
$$

$$
\overline{Q}_{22}^{(k)} = Q_{11}^{(k)}\sin^4\theta + Q_{22}^{(k)}\cos^4\theta + 2\left(Q_{12}^{(k)} + 2Q_{66}^{(k)}\right)\sin^2\theta\cos^2\theta
$$

$$
\overline{Q}_{12}^{(k)} = \left(Q_{11}^{(k)} + Q_{22}^{(k)} - Q_{66}^{(k)}\right)\sin^2\theta\cos^2\theta + Q_{12}^{(k)}\left(\cos^4\theta + \sin^4\theta\right)
$$

$$
\overline{Q}_{16}^{(k)} = \left(Q_{11}^{(k)} - Q_{12}^{(k)} - 2Q_{66}^{(k)}\right)\cos^3\theta\sin\theta - \left(Q_{22}^{(k)} - Q_{12}^{(k)} - 2Q_{66}^{(k)}\right)\sin^3\theta\cos\theta
$$

$$
\overline{Q}_{26}^{(k)} = \left(Q_{11}^{(k)} - Q_{12}^{(k)} - 2Q_{66}^{(k)}\right)\cos\theta\sin^3\theta - \left(Q_{22}^{(k)} - Q_{12}^{(k)} - 2Q_{66}^{(k)}\right)\sin\theta\cos^3\theta
$$

$$
\overline{Q}_{66}^{(k)} = \left(Q_{11}^{(k)} + Q_{22}^{(k)} - 2Q_{12}^{(k)} - 2Q_{66}^{(k)}\right)\cos^2\theta\sin^2\theta + Q_{66}^{(k)}\left(\sin^4\theta + \cos^4\theta\right)
$$

$$
\overline{Q}_{44}^{(k)} = Q_{55}^{(k)}\sin^2\theta + Q_{44}^{(k)}\cos^2\theta
$$

$$
\overline{Q}_{55}^{(k)} = Q_{55}^{(k)}\cos^2\theta + Q_{44}^{(k)}\sin^2\theta
$$

$$
\overline{Q}_{45}^{(k)} = \left(Q_{55}^{(k)} - Q_{44}^{(k)}\right)\cos\theta\sin\theta
$$

The equilibrium equations for conical shells of variable thickness after applying stress–strain relations (Equation (2)) are as follows:

$$
\begin{aligned}
&\left(A_{11}g\frac{\partial^2}{\partial x^2} + A_{11}\left(g' + g\frac{1}{x}\right)\frac{\partial}{\partial x} + A_{66}g\frac{1}{x^2\sin^2\alpha}\frac{\partial^2}{\partial \theta^2} + A_{12}g'\frac{1}{x} - A_{22}g\frac{1}{x^2}\right)U \\
&+\left((A_{12}+A_{66})g\frac{1}{x\sin\alpha}\frac{\partial^2}{\partial x\partial\theta} + \left(A_{12}g'\frac{1}{x\sin\alpha} - A_{22}g\frac{1}{x^2\sin\alpha} - A_{66}g\frac{1}{x^2\sin\alpha}\right)\frac{\partial}{\partial\theta}\right)V \\
&-\left(E_{11}c_2 g\frac{\partial^3}{\partial x^3} + \left(E_{11}c_2 g' - E_{11}c_2 g\frac{1}{x} + E_{12}c_2 g\frac{1}{x}\right)\frac{\partial^2}{\partial x^2} - A_{12}g\frac{1}{x\tan\alpha}\frac{\partial}{\partial x}\right. \\
&+\left(E_{12}c_2 g\frac{1}{x^2\sin^2\alpha} + 2E_{66}c_2 g\frac{1}{x^2\sin^2\alpha}\right)\frac{\partial^3}{\partial x\partial\theta^2} \\
&+\left(E_{12}c_2 g'\frac{1}{x^2\sin^2\alpha} - E_{12}c_2 g\frac{1}{x^3\sin^2\alpha} - E_{22}c_2 g\frac{1}{x^3\sin^2\alpha}\right)\frac{\partial^2}{\partial\theta^2} - \left(A_{12}g' - A_{22}g\frac{1}{x}\right)\frac{1}{x\tan\alpha}\right)W \\
&+\left((B_{11}-E_{11}c_2)g\frac{\partial^2}{\partial x^2} + (B_{11}-E_{11}c_2)\left(g' + g\frac{1}{x}\right)\frac{\partial}{\partial x}\right. \\
&+(B_{66}-E_{66}c_2)g\frac{1}{x^2\sin^2\alpha}\frac{\partial^2}{\partial\theta^2} + (B_{12}-E_{12}c_2)g'\frac{1}{x} - (B_{22}-E_{22}c_2)g\frac{1}{x^2}\right)\phi_x \\
&+\left((((B_{12}-E_{12}c_2) + (B_{66}-E_{66}c_2))g\frac{1}{x\sin\alpha}\frac{\partial^2}{\partial x\partial\theta} + (B_{12}-E_{12}c_2)g'\frac{1}{x\sin\alpha}\frac{\partial}{\partial\theta}\right. \\
&-(B_{22}-E_{22}c_2 + B_{66}-E_{66}c_2)g\frac{1}{x^2\sin\alpha}\frac{\partial}{\partial\theta}\right)\phi_\theta \\
&= I_0\ddot{u} + J_1\ddot{\phi}_x - c_1 I_3\frac{\partial\ddot{w}}{\partial x}
\end{aligned}
$$
(7a)

$$
\begin{aligned}
&\left((A_{66}+A_{12})g\frac{1}{x\sin\alpha}\frac{\partial^2}{\partial x\partial\theta} + \left(A_{66}\left(g'+g\frac{1}{x}\right)\frac{1}{x\sin\alpha} + A_{22}g\frac{1}{x^2\sin\alpha}\right)\frac{\partial}{\partial\theta}\right)U \\
&+\left(A_{66}g\frac{\partial^2}{\partial x^2} + A_{66}\left(g'+g\frac{1}{x}\right)\frac{\partial}{\partial x} + A_{22}g\frac{1}{x^2\sin^2\alpha}\frac{\partial^2}{\partial\theta^2} - A_{66}\left(g'+g\frac{1}{x}\right)\frac{1}{x} - (A_{44}-D_{44}c_1)g\frac{1}{x^2\tan^2\alpha}\right)V \\
&-\left((2E_{66}c_2+E_{12}c_2)g\frac{1}{x\sin\alpha}\frac{\partial^3}{\partial x^2\partial\theta} + \left(2E_{66}c_2\left(g'+g\frac{1}{x}\right)\frac{1}{x\sin\alpha}\right)\frac{\partial^2}{\partial x\partial\theta}\right. \\
&\left.+E_{22}c_2g\frac{1}{x^3\sin^3\alpha}\frac{\partial^3}{\partial\theta^3} - (A_{22}+A_{44}-D_{44}c_1)g\frac{1}{x^2\sin\alpha\tan\alpha}\frac{\partial}{\partial\theta}\right)W \\
&+\left(((B_{66}-E_{66}c_2)+(B_{12}-E_{12}c_2))g\frac{1}{x\sin\alpha}\frac{\partial^2}{\partial x\partial\theta}\right. \\
&\left.+\left((B_{66}-E_{66}c_2)\left(g'+g\frac{1}{x}\right)\frac{1}{x\sin\alpha} + (B_{22}-E_{22}c_2)g\frac{1}{x^2\sin\alpha}\right)\frac{\partial}{\partial\theta}\right)\phi_x \\
&+\left((B_{66}-E_{66}c_2)g\frac{\partial^2}{\partial x^2} + \left((B_{66}-E_{66}c_2)\left(g'+g\frac{2}{x}\right)\right)\frac{\partial}{\partial x} + (B_{22}-E_{22}c_2)g\frac{1}{x^2\sin^2\alpha}\frac{\partial^2}{\partial\theta^2}\right. \\
&\left.+(A_{44}-D_{44}c_1)g\frac{1}{x\tan\alpha} - (B_{66}-E_{66}c_2)\left(g'+g\frac{1}{x}\right)\frac{1}{x}\right)\phi_\theta \\
&= \left(I_0+\frac{2}{x\tan\alpha}I_1\right)\ddot v + \left(J_1+\frac{1}{x\tan\alpha}I_2 - c_1\frac{1}{x\tan\alpha}I_4\right)\ddot\phi_\theta - \left(c_1I_3+c_1\frac{1}{x\tan\alpha}I_4\right)\frac{\partial\ddot w}{\partial\theta}
\end{aligned}
$$

(7b)

$$
\begin{aligned}
&\left(E_{11}c_2g\frac{\partial^3}{\partial x^3} + \left(2E_{11}c_2g'+E_{12}c_2g\frac{1}{x}\right)\frac{\partial^2}{\partial x^2} - \left(A_{12}g\frac{1}{x\tan\alpha} - E_{11}c_2g'' - 2E_{12}c_2\left(g'-g\frac{1}{x}\right)\frac{1}{x}\right)\frac{\partial}{\partial x}\right. \\
&+\left(E_{12}c_2g\frac{1}{x^2\sin^2\alpha} + E_{66}c_2g\frac{2}{x^2\sin^2\alpha}\right)\frac{\partial^3}{\partial x\partial\theta^2} \\
&+\left(E_{22}c_2g\frac{1}{x^3\sin^2\alpha} + E_{66}c_2\left(g'-g\frac{1}{x}\right)\frac{1}{x^2\sin^2\alpha}\right)\frac{\partial^2}{\partial\theta^2} \\
&\left.-\left(A_{22}g\frac{1}{x^2\tan\alpha} - E_{12}c_2g''\frac{1}{x} + 2E_{12}g'\frac{1}{x^2} - E_{12}c_2g\frac{2}{x^3}\right)\right)U \\
&+\left(-E_{12}c_2g\frac{1}{x^2\sin\alpha}\frac{\partial^2}{\partial x^2} + \left(E_{12}c_2g''\frac{1}{x\sin\alpha} - 2E_{12}g'\frac{1}{x^2\sin\alpha} + E_{12}g'\frac{1}{x\sin\alpha} + E_{12}c_2g\frac{2}{x^3\sin\alpha}\right)\frac{\partial}{\partial x}\right. \\
&+\left(E_{66}c_2g\frac{2}{x\sin\alpha} + E_{12}c_2g\frac{1}{x\sin\alpha}\right)\frac{\partial^3}{\partial x^2\partial\theta} \\
&+\left(E_{66}c_2g'\frac{2}{x\sin\alpha} - E_{66}c_2g\frac{1}{x^2\sin\alpha} + E_{12}c_2\left(g'-g\frac{1}{x}\right)\frac{1}{x\sin\alpha}\right)\frac{\partial^2}{\partial x\partial\theta} + \left(E_{22}c_2g\frac{1}{x^3\sin^3\alpha}\right)\frac{\partial^3}{\partial\theta^3} \\
&\left.-\left((A_{44}-D_{44}c_1-D_{44}c_2+F_{44}c_1c_2-A_{22})g\frac{1}{x^2\sin\alpha\tan\alpha} - E_{66}c_2\left(g'-g\frac{1}{x}\right)\frac{2}{x^2\sin\alpha}\right)\frac{\partial}{\partial\theta}\right)V \\
&-\left(H_{11}c_2^2g\frac{\partial^4}{\partial x^4} + 2H_{11}c_2^2g'\frac{\partial^3}{\partial x^3}\right. \\
&-\left((A_{55}-D_{55}c_1-D_{55}c_2+F_{55}c_1c_2)g + E_{12}c_2g\frac{1}{x\tan\alpha} - H_{11}c_2^2g'' + E_{12}gc_2\frac{1}{x\tan\alpha}\right)\frac{\partial^2}{\partial x^2} \\
&-\left(2E_{12}c_2\left(g'-g\frac{1}{x}\right)\frac{1}{x\tan\alpha} + (A_{55}c_1-D_{55}c_1-D_{55}c_2+F_{55}c_1c_2)\left(g'+g\frac{1}{x}\right)\right)\frac{\partial}{\partial x} \\
&+\left(2H_{12}c_2^2g\frac{1}{x^2\sin^2\alpha} + 4H_{66}c_2^2g\frac{1}{x^2\sin^2\alpha}\right)\frac{\partial^4}{\partial x^2\partial\theta^2} \\
&+\left(4H_{66}c_2^2\left(g'-g\frac{1}{x}\right)\frac{1}{x^2\sin^2\alpha} + H_{12}c_2^2\left(g'-g\frac{2}{x}\right)\frac{1}{x^2\sin^2\alpha}\right)\frac{\partial^3}{\partial x\partial\theta^2} \\
&-\left((A_{44}-D_{44}c_1-D_{44}c_2+F_{44}c_1c_2)g\frac{1}{x^2\sin^2\alpha}\right)\frac{\partial^2}{\partial\theta^2} + \left(H_{22}c_2^2g\frac{1}{x^4\sin^4\alpha}\right)\frac{\partial^4}{\partial\theta^4} \\
&\left.+A_{22}g\frac{1}{x^2\tan^2\alpha} + E_{12}g''c_2\frac{1}{x\tan\alpha} - 2E_{12}c_2g'\frac{1}{x^2\tan\alpha} + E_{12}g\frac{2}{x^3\tan\alpha}\right)W \\
&+\left(\left(F_{11}c_2-H_{11}c_2^2\right)g\frac{\partial^3}{\partial x^3} + 2\left(F_{11}c_2-H_{11}c_2^2\right)g'\frac{\partial^2}{\partial x^2}\right. \\
&+\left((A_{55}-D_{55}c_1-D_{55}c_2+F_{55}c_1c_2)g - (B_{12}-E_{12}c_2)g\frac{1}{x\tan x} + (F_{11}c_2-H_{11}c_2^2)g''\right. \\
&\left.+2(F_{12}c_2-H_{12}c_2^2)\left(g'-g\frac{1}{x}\right)\frac{1}{x}\right)\frac{\partial}{\partial x} + \left((F_{22}c_2-H_{22}c_2^2)g\frac{1}{x^3\sin^2\alpha} + (F_{66}c_2-H_{66}c_2^2)g\frac{2}{x^2\sin^2\alpha}\right)\frac{\partial^3}{\partial x\partial\theta^2} \\
&+\left((F_{22}c_2-H_{22}c_2^2)g\frac{1}{x^3\sin^2\alpha} + (F_{66}c_2-H_{66}c_2^2)\left(g'-g\frac{1}{x}\right)\frac{2}{x^2\sin^2\alpha}\right)\frac{\partial^2}{\partial\theta^2} \\
&+(A_{55}-D_{55}c_1-D_{55}c_2+F_{55}c_1c_2)\left(g'+g\frac{1}{x}\right) - (B_{22}-E_{22}c_2)g\frac{1}{x^2\tan\alpha} \\
&\left.+(F_{12}c_2-H_{12}c_2^2)g''\frac{1}{x} - 2(F_{12}c_2-H_{12}c_2^2)g'\frac{1}{x^2} + (F_{12}c_2-H_{12}c_2^2)g\frac{2}{x^3}\right)\phi_x \\
&+\left(\left((F_{66}c_2-H_{66}c_2^2)g\frac{2}{x\sin\alpha} + (F_{12}c_2-H_{12}c_2^2)g\frac{1}{x\sin\alpha}\right)\frac{\partial^3}{\partial x^2\partial\theta}\right. \\
&+\left((F_{66}c_2-H_{66}c_2^2)g'\frac{2}{x\sin\alpha} - (F_{66}c_2-H_{66}c_2^2)g\frac{2}{x^2\sin\alpha} + 2(F_{12}c_2-H_{12}c_2^2)\left(g'-g\frac{1}{x}\right)\frac{1}{x\sin\alpha}\right)\frac{\partial^2}{\partial x\partial\theta} \\
&+\left((F_{22}c_2-H_{22}c_2^2)g\frac{1}{x^3\sin^3\alpha}\right)\frac{\partial^3}{\partial\theta^3} + \left((A_{44}-D_{44}c_1-D_{44}c_2+F_{44}c_1c_2)g\frac{1}{x\sin\alpha}\right. \\
&-(B_{22}-E_{22}c_2)g\frac{1}{x^2\sin\alpha\tan\alpha} - (F_{66}c_2-H_{66}c_2^2)\left(g'-g\frac{1}{x}\right)\frac{2}{x^2\sin\alpha} \\
&\left.\left.+(F_{12}c_2-H_{12}c_2^2)g''\frac{1}{x\sin\alpha} - 2(F_{12}c_2-H_{12}c_2^2)g'\frac{1}{x^2\sin\alpha} + (F_{12}c_2-H_{12}c_2^2)g\frac{2}{x^3\sin\alpha}\right)\frac{\partial}{\partial\theta}\right)\phi_\theta \\
&= c_1I_3\frac{\partial\ddot u}{\partial x} + \left(c_1I_3+\frac{c_1}{x\tan\alpha}I_4\right)\frac{\partial\ddot v}{\partial\theta} + I_0\ddot w - c_1^2I_6\left(\frac{\partial^2\ddot w}{\partial x^2}+\frac{\partial^2\ddot w}{\partial\theta^2}\right) \\
&+c_1J_4\frac{\partial\ddot\phi_x}{\partial x} + c_1J_4\frac{\partial\ddot\phi_\theta}{\partial\theta}
\end{aligned}
$$

(7c)

$$
\begin{aligned}
&\left((B_{11} - E_{11}c_1)g\frac{\partial^2}{\partial x^2} + \left((B_{11} - E_{11}c_1)\left(g' + g\frac{1}{x} \right) \right)\frac{\partial}{\partial x} + \left((B_{66} - E_{66}c_1)g\frac{1}{x^2\sin^2\alpha} \right)\frac{\partial^2}{\partial\theta^2} \right. \\
&\left. + (B_{12} - E_{12}c_1)g'\frac{1}{x} - (B_{22} - E_{22}c_1)g\frac{1}{x^2} \right)U \\
&+ \left(\left(((B_{12} - E_{12}c_1) + (B_{66} - E_{66}c_1))g\frac{1}{x\sin\alpha} \right)\frac{\partial^2}{\partial x\partial\theta} \right. \\
&\left. + \left((B_{12} - E_{12}c_1)g'\frac{1}{x\sin\alpha} - (B_{22} - E_{22}c_1)g\frac{1}{x^2\sin\alpha} - (B_{66} - E_{66}c_1)g\frac{1}{x^2\sin\alpha} \right)\frac{\partial}{\partial\theta} \right)V \\
&- \left((F_{11}c_2 - H_{11}c_1c_2)g\frac{\partial^3}{\partial x^3} + \left((F_{11}c_2 - H_{11}c_1c_2)g' + (F_{11}c_2 - H_{11}c_1c_2)g\frac{1}{x} + (F_{12}c_2 - H_{12}c_1c_2)g\frac{1}{x} \right)\frac{\partial^2}{\partial x^2} \right. \\
&- \left((B_{12} - E_{12}c_1)g\frac{1}{x\tan\alpha} - ((A_{55} - D_{55}c_1 - D_{55}c_2 + F_{55}c_1c_2)g)) \right)\frac{\partial}{\partial x} \\
&+ \left((F_{12}c_2 - H_{12}c_1c_2) + 2(F_{66}c_2 - H_{66}c_1c_2)g\frac{1}{x^2\sin^2\alpha} \right)\frac{\partial^3}{\partial x\partial\theta^2} \\
&+ \left((F_{12}c_2 - H_{12}c_1c_2)\left(g' - g\frac{1}{x} \right)\frac{1}{x^2\sin^2\alpha} - (F_{22}c_2 - H_{22}c_1c_2)g\frac{1}{x^3\sin^2\alpha} \right)\frac{\partial^2}{\partial\theta^2} \\
&\left. - (B_{12} - E_{12}c_1)g'\frac{1}{x\tan\alpha} + (B_{22} - E_{22}c_1)g\frac{1}{x^2\tan\alpha} \right)W \\
&+ \left(((D_{11} - F_{11}c_2 - F_{11}c_1 + H_{11}c_1c_2)g)\frac{\partial^2}{\partial x^2} + \left((D_{11} - F_{11}c_2 - F_{11}c_1 + H_{11}c_1c_2)\left(g' + g\frac{1}{x} \right) \right)\frac{\partial}{\partial x} \right. \\
&+ \left((D_{66} - F_{66}c_2 - F_{66}c_1 + H_{66}c_1c_2)g\frac{1}{x^2\sin^2\alpha} \right)\frac{\partial^2}{\partial\theta^2} \\
&+ (D_{12} - F_{12}c_2 - F_{12}c_1 + H_{12}c_1c_2)g'\frac{1}{x} - (D_{22} - F_{22}c_2 - F_{22}c_1 + H_{22}c_1c_2)g\frac{1}{x^2} \\
&\left. - (A_{55} - D_{55}c_1 - D_{55}c_2 + F_{55}c_1c_2)g \right)\phi_x \\
&+ \left(((D_{12} - F_{12}c_2 - F_{12}c_1 + H_{12}c_1c_2) + (D_{66} - F_{66}c_2 - F_{66}c_1 + H_{66}c_1c_2))g\frac{1}{x\sin\alpha}\frac{\partial^2}{\partial x\partial\theta} \right. \\
&+ (D_{12} - F_{12}c_2 - F_{12}c_1 + H_{12}c_1c_2)g'\frac{1}{x\sin\alpha}\frac{\partial}{\partial\theta} - (D_{22} - F_{22}c_2 - F_{22}c_1 + H_{22}c_1c_2)g\frac{1}{x^2\sin\alpha}\frac{\partial}{\partial\theta} \\
&\left. - (D_{66} - F_{66}c_2 - F_{66}c_1 + H_{66}c_1c_2)g\frac{1}{x^2\sin\alpha}\frac{\partial}{\partial\theta} \right)\phi_\theta \\
&= J_1\ddot{u} - c_1J_4\frac{\partial\ddot{w}}{\partial x} + K_2\ddot{\phi}_x
\end{aligned}
\tag{7d}
$$

$$
\begin{aligned}
&\left(\left(((B_{66} - E_{66}c_1) + (B_{12} - E_{12}c_1))g\frac{1}{x\sin\alpha} \right)\frac{\partial^2}{\partial x\partial\theta} \right. \\
&\left. + \left((B_{66} - E_{66}c_1)\left(g' + g\frac{1}{x} \right)\frac{1}{x\sin\alpha} + (B_{22} - E_{22}c_1)g\frac{1}{x^2\sin\alpha} \right)\frac{\partial}{\partial\theta} \right)U \\
&+ \left((B_{66} - E_{66}c_1)g + (B_{22} - E_{22}c_1)g\frac{1}{x^2\sin^2\alpha} \right)\frac{\partial^2}{\partial x^2} + \left((B_{66} - E_{66}c_1)\left(g' + g\frac{1}{x} \right) \right)\frac{\partial}{\partial x} \\
&- (B_{66} - E_{66}c_1)\left(g' + g\frac{1}{x} \right)\frac{1}{x} - (A_{44} - D_{44}c_1 - D_{44}c_2 + F_{44}c_1c_2)g\frac{1}{x\tan\alpha} \bigg) V \\
&- \left(\left((2(F_{66}c_2 - H_{66}c_1c_2) + (F_{12}c_2 - H_{12}c_1c_2))g\frac{1}{x\sin\alpha} \right)\frac{\partial^3}{\partial x^2\partial\theta} + \left(2(F_{66}c_2 - H_{66}c_1c_2)\left(g' + g\frac{1}{x} \right)\frac{1}{x\sin\alpha} \right)\frac{\partial^2}{\partial x\partial\theta} \right. \\
&+ (F_{12}c_2 - H_{12}c_1c_2)g\frac{1}{x^3\sin^3\alpha}\frac{\partial^3}{\partial\theta^3} \\
&\left. - \left((B_{22} - E_{22}c_1)g\frac{1}{x^2\sin\alpha\tan\alpha} - (A_{44} - D_{44}c_1 - D_{44}c_2 + F_{44}c_1c_2)g\frac{1}{x\sin\alpha} \right)\frac{\partial}{\partial\theta} \right)W \\
&+ \left(((D_{66} - F_{66}c_2 - F_{66}c_1 + H_{66}c_1c_2) + (D_{12} - F_{12}c_2 - F_{12}c_1 + H_{12}c_1c_2))g\frac{1}{x\sin\alpha}\frac{\partial^2}{\partial x\partial\theta} \right. \\
&\left. + \left((D_{66} - F_{66}c_2 - F_{66}c_1 + H_{66}c_1c_2)\left(g' + g\frac{1}{x} \right)\frac{1}{x\sin\alpha} + (D_{22} - F_{22}c_2 - F_{22}c_1 + H_{22}c_1c_2)g\frac{1}{x^2\sin\alpha} \right)\frac{\partial}{\partial\theta} \right)\phi_x \\
&+ ((D_{66} - F_{66}c_2 - F_{66}c_1 + H_{66}c_1c_2)g\frac{\partial^2}{\partial x^2} \\
&+ (D_{66} - F_{66}c_2 - F_{66}c_1 + H_{66}c_1c_2)\left(g' + g\frac{1}{x} \right)\frac{\partial}{\partial x} \\
&+ \left((D_{22} - F_{22}c_2 - F_{22}c_1 + H_{22}c_1c_2)g\frac{1}{x^2\sin^2\alpha} \right)\frac{\partial^2}{\partial\theta^2} \\
&- (D_{66} - F_{66}c_2 - F_{66}c_1 + H_{66}c_1c_2)\left(g' + g\frac{1}{x} \right)\frac{1}{x} - (A_{44}c_1 - D_{44}c_1 - D_{44}c_2 + F_{44}c_1c_2)g)\phi_\theta \\
&= \left(J_1 + \frac{1}{x\tan\alpha}I_2 - c_1\frac{1}{x\tan\alpha}I_4 \right)\ddot{v} - c_1J_4\frac{\partial\ddot{w}}{\partial\theta} + K_2\ddot{\phi}_\theta
\end{aligned}
\tag{7e}
$$

$$\alpha \text{ is the cone angle}$$

$$\overline{M}_x = M_x - c_1P_x,\ \overline{M}_\theta = M_\theta - c_1P_\theta,\ \overline{M}_{x\theta} = M_{x\theta} - c_1P_{x\theta}$$

$$\overline{Q}_\theta = Q_\theta - c_2R_\theta,\ \overline{Q}_x = Q_x - c_2R_x$$

$$J_1 = I_1 - c_1I_3,$$

$$J_4 = I_4 - c_1I_6,$$

$$K_2 = I_2 - 2c_1I_4 + c_1^2I_6$$

The displacements and rotational functions are assumed in the cos and sine functions.
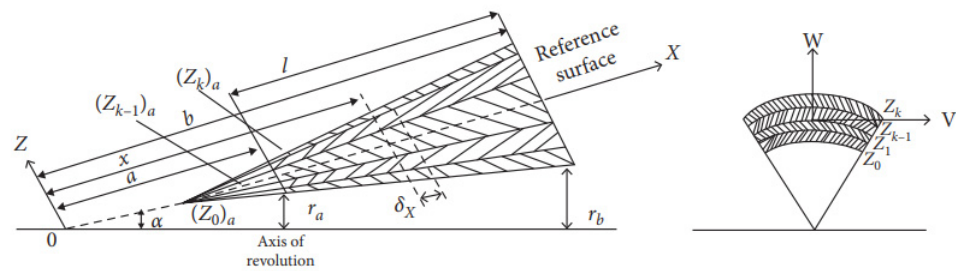
Figure 2. Layered conical shell of variable thickness.

The non-dimensional parameters are as follows:

$$
\begin{aligned}
&X = \tfrac{x-a}{l}, \ a \le x \le b \ and \ X \in [0,1] \\
&\lambda = \omega l \sqrt{\tfrac{I_1}{A_{11}}}, \text{ a frequency parameter} \\
&\beta = \tfrac{a}{b}, \text{ the length ratio} \\
&\gamma = \tfrac{h_0}{r_q}, \ \gamma' = \tfrac{h_0}{a}, \text{ ratios of thickness to radius and to a length} \\
&\delta_k = \tfrac{h_k}{h}, \text{ the relative layer thickness of the k-th layer}
\end{aligned}
\tag{8}
$$

The three types of thickness variations considered are as follows.

Case (i):

If $C_e = C_s = 0$, then the thickness variation becomes linear. In this case it can be easily shown that
$C_\ell = \tfrac{1}{\eta} - 1$, where η is the taper ratio $h_k(0)/h_k(1)$.

Case (ii):

If $C_\ell = C_s = 0$, then the thickness varies exponentially.

Case (iii):

If $C_\ell = C_e = 0$, then the thickness varies sinusoidally.
It may be noted that the thickness of any layer at the end is $X = 0$ is h_{0k} for cases (i) and (iii), but is $h_{0k}(1 + C_e)$ for case (ii).
The thickness variation of the kth layer of the shell is assumed in the form as

$$
h_k(x) = h_{0k} \, g(x)
$$

where

$$
g(x) = 1 + C_\ell \left(\frac{x - x_a}{\ell} \right) + C_e \exp\left(\frac{x - x_a}{\ell} \right) + C_s \sin \pi \left(\frac{x - x_a}{\ell} \right),
$$

where h_{0k} is a constant thickness of the kth layer, $\ell = b - a$ is the length of the cone and x_a is the distance from the origin to $x = a$ (small end of the cone). The thickness of the shell becomes uniform when $g(x) = 1$.

Since the thickness is assumed to be varying along the axial direction, one can define the elastic coefficients A_{ij}, B_{ij} and D_{ij} (extensional, bending–extensional coupling and bending stiffnesses) and higher-order stiffness coefficients E_{ij}, F_{ij} and H_{ij} corresponding to layers of uniform thickness with superscript 'c'.

$$
A_{ij} = A_{ij}^c \, g(x), \ B_{ij} = B_{ij}^c \, g(x), \ D_{ij} = D_{ij}^c \, g(x), E_{ij} = E_{ij}^c \, g(x), \ F_{ij} = F_{ij}^c \, g(x), H_{ij} = H_{ij}^c \, g(x)
$$

Method of Solution

The differential equations obtained are approximated by using cubic and quantic spline functions, in the range of $X \in [0,1]$.

Displacements $U(X)$, $V(X)$ and $W(X)$ and rotational functions $\Phi_X(X)$, $\Phi_\theta(X)$ are approximated, respectively, by the splines Refs. [30–33].

$$U(X) = \sum_{i=0}^{4} a_i X^i + \sum_{j=0}^{N-1} b_j(X - X_j)^5 H(X - X_j)$$
$$V(X) = \sum_{i=0}^{2} c_i X^i + \sum_{j=0}^{N-1} d_j(X - X_j)^3 H(X - X_j)$$
$$W(X) = \sum_{i=0}^{4} e_i X^i + \sum_{j=0}^{N-1} f_j(X - X_j)^5 H(X - X_j) \quad (9)$$
$$\Phi_X(X) = \sum_{i=0}^{4} g_i X^i + \sum_{j=0}^{N-1} g_j(X - X_j)^5 H(X - X_j)$$
$$\Phi_\theta(X) = \sum_{i=0}^{2} l_i X^i + \sum_{j=0}^{N-1} q_j(X - X_j)^3 H(X - X_j)$$

where a_i, c_i, e_i, g_i, l_i, b_i, d_i, f_i, p_i and q_i are unknown coefficients (i.e., spline coefficients), $H(X - X_j)$ is the Heaviside step function and N is the number of intervals into which the range $[0, 1]$ of X is divided. The points $X = X_s = \frac{s}{N}$, $(s = 0, 1, 2 \ldots N)$ are chosen as the knots of the splines, as well as the collocation points. Thus, the splines are assumed to satisfy the differential equations at all X_s. The resulting expressions contain $(5N + 5)$ a homogeneous system of equations in the $(5N + 21)$ spline coefficients.

The simply supported boundary condition is considered.

This boundary condition gives 13 more equations, thus making a total of $(5N + 18)$ equations, with the same number of unknowns. The resulting field and boundary condition equations may be written in the form

$$[M]\{q\} = \lambda^2[P]\{q\} \quad (10)$$

where $[M]$ and $[P]$ are square matrices, and $\{q\}$ is a column matrix. This is treated as a generalised eigenvalue problem in the eigenfrequency parameter λ and the eigenvector $\{q\}$, whose elements are the spline coefficients. It is solved for the first three eigenvalues, giving the corresponding frequency parameters, and the related eigenvectors from which the mode shapes can be constructed. The square matrices consist of stress, strain and displacement components effecting the frequency parameter value.

3. Results and Discussion

In this present study, the conical shells consisted of Kevlar Epoxy and Graphite Epoxy layers. Shells with two, three, four, five and six symmetric cross-ply layers were considered. The effects of the three different types of thicknesses (such as linear, sinusoidal and exponential) on the frequency value were examined.

The elastic properties of Kevlar Epoxy and Graphite Epoxy are given in Table 1.

Table 1. Elastic properties of materials used.

Elastic Property	Density $\times 10^3 \text{N}-\text{s}^2/\text{m}^4$	Young Modulus $E_x \times 10^{10} \text{N}/\text{m}^2$	Young Modulus $E_y \times 10^{10} \text{N}/\text{m}^2$	Shear Modulus $G_{xz} \times 10^{10} \text{N}/\text{m}^2$	Shear Modulus $G_{yz} \times 10^{10} \text{N}/\text{m}^2$	Shear Modulus $G_{xy} \times 10^{10} \text{N}/\text{m}^2$	Major Poisson Ratio, υ_{xy}
Graphite Epoxy	2550	11.72	42.75	4.14	3.45	4.14	0.27
Kevlar Epoxy	1770	9.65	144.8	4.14	3.45	4.14	0.30

Table 2 shows the comparison of this present study with Irie et al. [34], Liew et al. [35] and Dai et al. [36]. It is evident from the results that the present results are very close to the already existing literature.

Table 2. Comparison of frequency parameter of present study with Refs. [34–36].

n	α=30°				α=60°			
	Ref. [34]	**Ref. [35]**	**Ref. [36]**	**Present**	**Ref. [34]**	**Ref. [35]**	**Ref. [36]**	**Present**
1	0.5923	-	0.5922	0.5921	0.4754	-	0.4754	0.4753
2	0.7910	0.7909	0.7909	0.7908	0.5722	0.5719	0.5721	0.5720
3	0.7284	0.7281	0.7282	0.7281	0.6001	0.5998	0.6001	0.6000
4	0.6352	0.6347	0.6349	0.6348	0.6054	0.6049	0.6053	0.6052
5	0.5531	0.5522	0.5525	0.5524	0.6077	0.6071	0.6075	0.6074
6	0.4949	0.4938	0.4941	0.4940	0.6159	0.6152	0.6156	0.6155
7	0.4653	0.4639	0.4643	0.4642	0.6343	0.6335	0.6340	0.6339
8	0.4654	0.4629	0.4633	0.4632	0.6650	0.6641	0.6646	0.6645
9	0.4892	0.4875	0.4879	0.4878	0.7084	0.7075	0.7080	0.7079

Table 3 shows a comparison of this present study (linear thickness variation and constant thickness) with Kumar et al. [37] (constant thickness). It is concluded that shells with non-uniform thickness have lower frequency value compared to shells with constant thickness. Lower frequencies are often preferred as they indicate larger, more global modes of vibration, which are typically easier to control and maintain the stability of the structure. The data comparisons in Tables 3 and 4 show that the frequency parameter value is significantly less for shells of non-uniform thickness compared to shell of constant thickness. The deviation in the results is due to the non-uniform thickness formulation. It is evident from the results that the shells of non-uniform thickness are less stiff, but more flexible and stable compared to shells of constant thickness.

Table 3. Comparison of non-dimensional frequency parameter of present study $\lambda = \omega \ell \sqrt{\frac{I_0}{A_{11}}}$ with Kumar et al. [37] $\overline{\omega} = \frac{\omega a^2}{h} \sqrt{\frac{\rho}{E_2}}$.

θ	α	0/θ/0			0/θ/0/θ			0/θ/θ/0		
		Ref. [37] Constant Thickness	**Ref. [29] Constant Thickness**	**Present Non-Uniform Thickness (Linear)**	**Ref. [37] Constant Thickness**	**Ref. [29] Constant Thickness**	**Present Non-Uniform Thickness (Linear)**	**Ref. [37] Constant Thickness**	**Ref. [29] Constant Thickness**	**Present Non-Uniform Thickness (Linear)**
90°	15°	40.0104	39.2930	38.1350	46.9078	45.9213	44.8321	43.0824	42.4646	41.2301
	30°	40.7529	41.7195	40.0167	53.0184	54.7141	53.1856	45.1971	46.8699	45.1028
	45°	47.1356	46.4112	45.3290	67.3628	66.4144	65.3421	54.2594	53.4415	52.1206

Table 4. Comparison of fundamental angular frequency ω with respect to length ratio β of constant and variable thickness of 6-layered shells for $n = 2$, $\gamma = 0.05$ for different cone angles for simply supported end conditions.

β	α=30°		α=45°		α=60°	
	Ref. [29] Constant Thickness	**Present Non-Uniform Thickness (Linear)**	**Ref. [29] Constant Thickness**	**Present Non-Uniform Thickness (Linear)**	**Ref. [29] Constant Thickness**	**Present Non-Uniform Thickness (Linear)**
0.1	0.77668	0.47835	1.42325	1.63228	1.62430	1.54407
0.3	1.95024	0.67658	3.04714	1.81080	4.10529	1.73537
0.5	3.92301	2.04632	4.10978	2.23309	5.32410	2.70950
0.7	6.02111	3.79282	6.26694	3.61209	6.44491	3.79006
0.9	19.28013	9.05599	21.3657	11.16722	27.23109	17.14523

In Table 4, a comparative study was conducted for the effect of length ratios on angular frequency values of different cone angles of shells of constant and non-uniform

thickness. Shells with non-uniform thickness have lower angular frequency values than the shells with constant thickness. Our objective to obtain lower frequency was achieved through this result as well. Moreover, a comparison of constant and non-uniform thickness shells by varying cone angle is shown in Table 5. Table 6 shows that the influence of exponential thickness variation on the frequency parameter. It was observed that as the layers of conical shells increase, the frequency value decreases. The same trend can be seen in Table 7, where the relationship is shown between sinusoidal thickness variation and the frequency parameter. In Table 8, the effect of linear thickness variation on the frequency parameter is shown. If we compare Tables 6–8, the differences in the values of the frequency parameter is very small, but the fact is, a marginal difference is significant for engineers while constructing stable structures. The value of the frequency parameter is higher for three-layered shells than for two-layered shell. Otherwise, four- to six-layered shell frequency parameter values lower as the number of layers increases. The results given in Tables 2–8 show that as the number of layers of conical shells increases, the frequency values decrease. Moreover, by varying the length ratios and cone angles, shells with non-uniform thickness have lower frequency values compared to shells of constant thickness. So, our objective to achieve lower frequency values was fulfilled by non-uniform thickness and increasing the number of layers of shells. In conclusion, our results evidently show the appropriateness of the methodology used.

Table 5. Comparison of frequency parameter λ_m, $m = 1, 2, 3$ with respect to cone angle α of constant and variable thickness of 5-layered conical shells for $n = 2$, $\gamma' = 0.5$ and $\beta = 0.3$ for simply supported end conditions.

α	Ref. [29] λ_1 Constant Thickness	Present λ_1 Non-Uniform Thickness (Linear)	Ref. [29] λ_2 Constant Thickness	Present λ_2 Non-Uniform Thickness (Linear)	Ref. [29] λ_3 Constant Thickness	Present λ_3 Non-Uniform Thickness (Linear)
10	0.00674	0.005735	0.00799	0.004567	0.01011	0.006426
20	0.00481	0.003271	0.00599	0.003650	0.00677	0.005544
30	0.00370	0.002364	0.00460	0.002321	0.00516	0.0040231
40	0.00354	0.002071	0.00418	0.001802	0.00481	0.0037220
50	0.00346	0.001958	0.00402	0.001737	0.00458	0.003413
60	0.00345	0.001933	0.00402	0.001737	0.00446	0.0033210
70	0.00346	0.001931	0.00401	0.001701	0.00445	0.003311
80	0.00344	0.001803	0.00403	0.001700	0.00439	0.0032210

Table 6. Effect of coefficient of exponential variation in thickness on fundamental frequency parameter of two- to six-layered shells.

Ce	2-Layered (0°/90°) (Graphite Epoxy/Kevlar Epoxy)	3-Layered (0°/90°/0°) (Graphite Epoxy/Kevlar Epoxy/Graphite Epoxy)	4-Layered (0°/90°/0°/90°) (Graphite Epoxy/Kevlar Epoxy/Graphite Epoxy/Kevlar Epoxy)	5-Layered (0°/90°/0°/90°/0°) (Graphite Epoxy/Kevlar Epoxy/Graphite Epoxy/Kevlar Epoxy/Graphite Epoxy)	6-Layered (0°/90°/0°/90°/0°/90°) (Graphite Epoxy/Kevlar Epoxy/Graphite Epoxy/Kevlar Epoxy/Graphite Epoxy/Kevlar Epoxy)
−0.2	0.024284	0.019866	0.018463	0.016177	0.015243
−0.1	0.024294	0.019866	0.017913	0.016155	0.015109
0	0.024294	0.019663	0.017823	0.016536	0.015091
0.1	0.024243	0.019726	0.018012	0.016172	0.015149
0.2	0.024281	0.019874	0.018513	0.016078	0.014964
−0.2	0.024284	0.019866	0.018463	0.016177	0.015243

Table 7. Effect of coefficient of sinusoidal variation in thickness on fundamental frequency parameter of two- to six-layered shells.

Cs	2-Layered (0°/90°) (Graphite Epoxy/Kevlar Epoxy)	3-Layered (0°/90°/0°) (Graphite Epoxy/Kevlar Epoxy/Graphite Epoxy)	4-Layered (0°/90°/0°/90°) (Graphite Epoxy/Kevlar Epoxy/Graphite Epoxy/Kevlar Epoxy)	5-Layered (0°/90°/0°/90°/0°) (Graphite Epoxy/Kevlar Epoxy/Graphite Epoxy/Kevlar Epoxy/Graphite Epoxy)	6-Layered (0°/90°/0°/90°/0°/90°) (Graphite Epoxy/Kevlar Epoxy/Graphite Epoxy/Kevlar Epoxy/Graphite Epoxy/Kevlar Epoxy)
−0.5	0.020274	0.01824	0.017201	0.016536	0.015149
−0.3	0.020284	0.01824	0.017231	0.016536	0.015149
−0.1	0.020264	0.01824	0.017221	0.016536	0.015149
0.1	0.020284	0.01824	0.017225	0.016536	0.015149
0.3	0.020284	0.01824	0.017246	0.016536	0.015149
0.5	0.020284	0.01824	0.017218	0.016536	0.015149

Table 8. Effect of coefficient of linear variation in thickness on fundamental frequency parameter of two- to six-layered shells.

η	2-Layered (0°/90°) (Graphite Epoxy/Kevlar Epoxy)	3-Layered (0°/90°/0°) (Graphite Epoxy/Kevlar Epoxy/Graphite Epoxy)	4-Layered (0°/90°/0°/90°) (Graphite Epoxy/Kevlar Epoxy/Graphite Epoxy/Kevlar Epoxy)	5-Layered (0°/90°/0°/90°/0°) (Graphite Epoxy/Kevlar Epoxy/Graphite Epoxy/Kevlar Epoxy/Graphite Epoxy)	6-Layered (0°/90°/0°/90°/0°/90°) (Graphite Epoxy/Kevlar Epoxy/Graphite Epoxy/Kevlar Epoxy/Graphite Epoxy/Kevlar Epoxy)
0.5	0.018621	0.019896	0.016996	0.01541	0.009996
0.7	0.018913	0.019858	0.017117	0.01542	0.010095
0.9	0.018824	0.019841	0.016929	0.01542	0.010118
1.1	0.018503	0.019741	0.017135	0.01543	0.010309
1.3	0.018615	0.019723	0.016946	0.01543	0.010055
1.5	0.018712	0.019625	0.016898	0.01541	0.010134
1.7	0.018804	0.019804	0.017271	0.01543	0.01006
1.9	0.018973	0.019863	0.017399	0.01542	0.009997
2.1	0.018626	0.019771	0.016715	0.01541	0.010214

Figure 3a–c depicts the effect of three different thickness variations (linear, exponential and sinusoidal) on the frequency parameter of three-layered shells (0°/90°/0°; Graphite Epoxy/Kevlar Epoxy/Graphite Epoxy). The effect of length ratio on the fundamental angular frequency parameter of two- to six-layered shells are shown in Figure 4. The effect of cone angle on the frequency parameter of five- and six-layered conical shells can be seen in Figure 5, under linear thickness variation, in Figure 6, under exponential thickness variation, and Figure 7, under sinusoidal thickness variation. Moreover, the influence of circumferential node number on the frequency parameter of five- and six-layered (0°/90°/0°/90°/0°; Graphite Epoxy/Kevlar Epoxy/Graphite Epoxy/Kevlar Epoxy/Graphite Epoxy) and (0°/90°/0°/90°/0°/90°; Graphite Epoxy/Kevlar Epoxy/Graphite Epoxy/Kevlar Epoxy/ Graphite Epoxy/Kevlar Epoxy) conical shells under linear thickness variation, exponential thickness variation and sinusoidal thickness variation can be seen in Figures 8–10, respectively. Figure 11 depicts the circumferential vibration form for *n* = 2, 3 and 4.
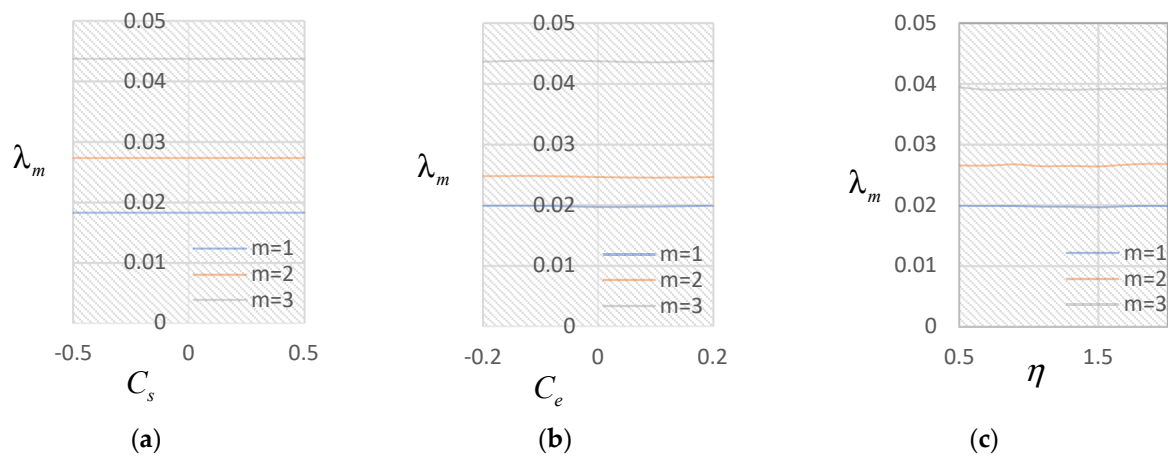
Figure 3. Effect of three thickness variations ((**a**) sinusoidal, (**b**) exponential and (**c**) linear) on the frequency parameter.
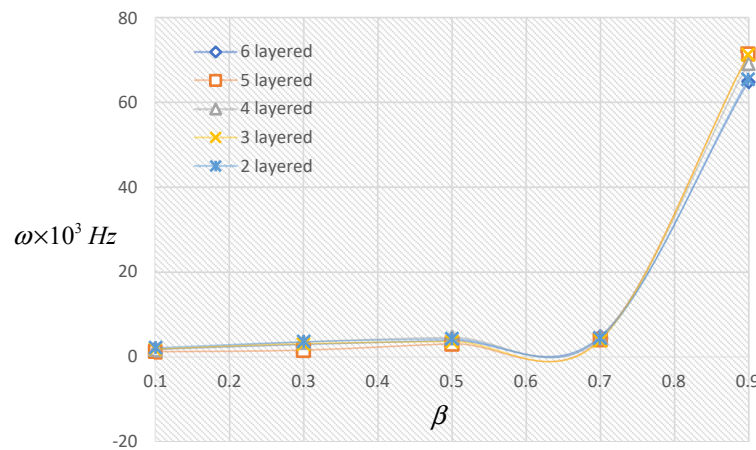
Figure 4. Effect of length ratio on the angular frequency parameter.
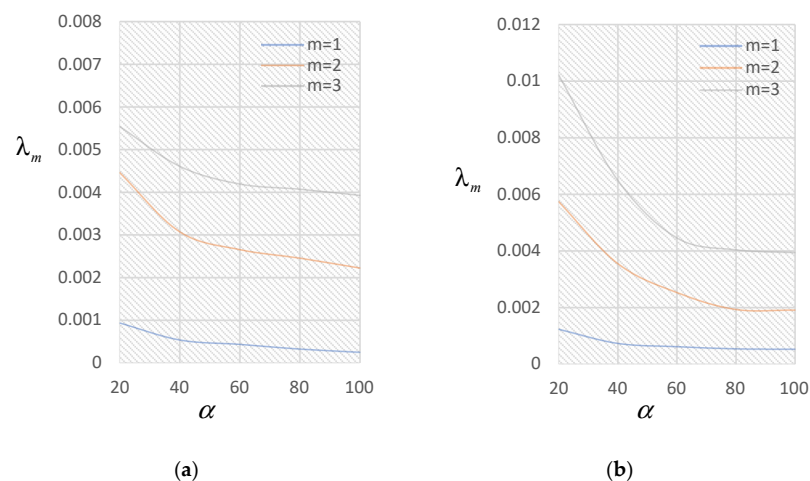
Figure 5. Effect of cone angle on the frequency parameter. (**a**) Five-layered $(0^0/90^0/0^0/90^0/0^0)$ Graphite Epoxy/Kevlar Epoxy/Graphite Epoxy/Kevlar Epoxy/Graphite Epoxy. (**b**) Six-layered $(0°/90°/0°/90°/0°/90°)$ Graphite Epoxy/Kevlar Epoxy/Graphite Epoxy/Kevlar Epoxy/Graphite Epoxy/Kevlar Epoxy shells under the effect of linear thickness variation.

(a)

(b)
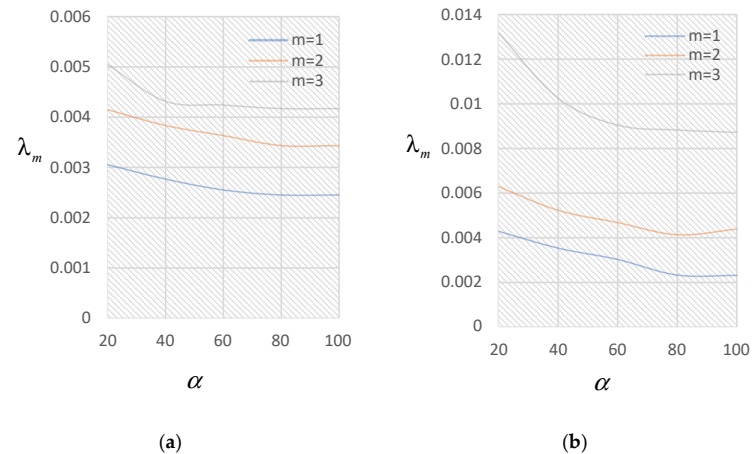
Figure 6. Effect of cone angle on the frequency parameter. (**a**) Five-layered ($0°/90°/0°/90°/0°$) Graphite Epoxy/Kevlar Epoxy/Graphite Epoxy/Kevlar Epoxy/Graphite Epoxy. (**b**) Six-layered ($0°/90°/0°/90°/0°/90°$) Graphite Epoxy/Kevlar Epoxy/Graphite Epoxy/Kevlar Epoxy/Graphite Epoxy/Kevlar Epoxy shells under the effect of exponential thickness variation.

(a)

(b)
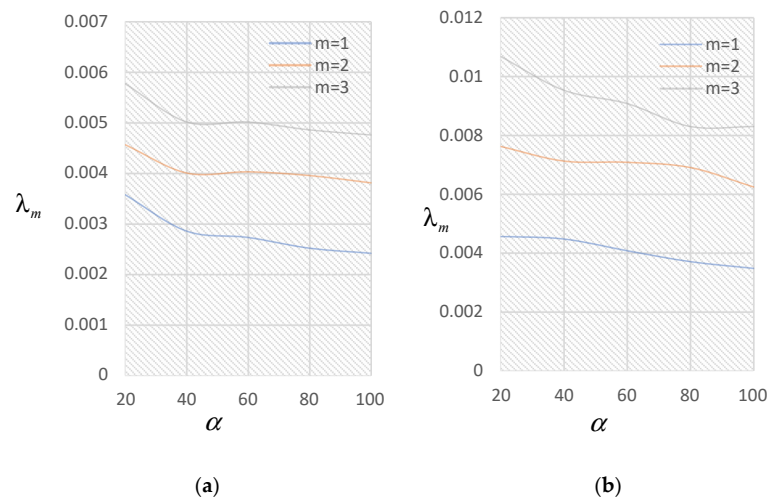
Figure 7. Effect of cone angle on the frequency parameter. (**a**) Five-layered ($0°/90°/0°/90°/0°$) Graphite Epoxy/Kevlar Epoxy/Graphite Epoxy/Kevlar Epoxy/Graphite Epoxy. (**b**) Six-layered ($0°/90°/0°/90°/0°/90°$) Graphite Epoxy/Kevlar Epoxy/Graphite Epoxy/Kevlar Epoxy/Graphite Epoxy/Kevlar Epoxy shells under the effect of sinusoidal thickness variation.

(a)

(b)
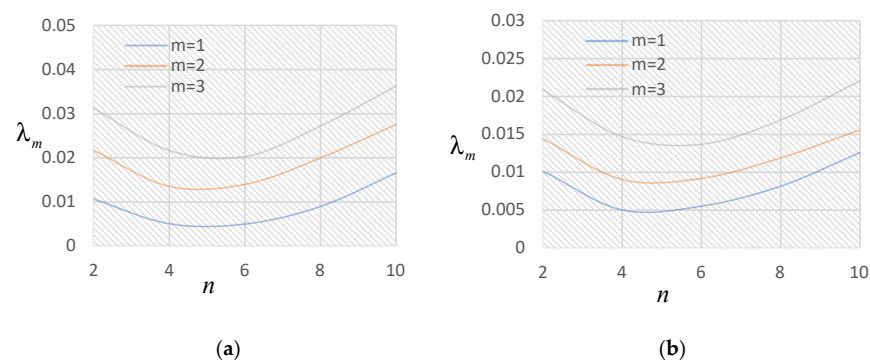
Figure 8. Effect of circumferential node number on the frequency parameter. (**a**) Five-layered ($0°/90°/0°/90°/0°$) Graphite Epoxy/Kevlar Epoxy/Graphite Epoxy/Kevlar Epoxy/Graphite Epoxy. (**b**) Six-layered ($0°/90°/0°/90°/0°/90°$) Graphite Epoxy/Kevlar Epoxy/Graphite Epoxy/Kevlar Epoxy/Graphite Epoxy/Kevlar Epoxy shells under the effect of linear thickness variation.

(**a**) (**b**)
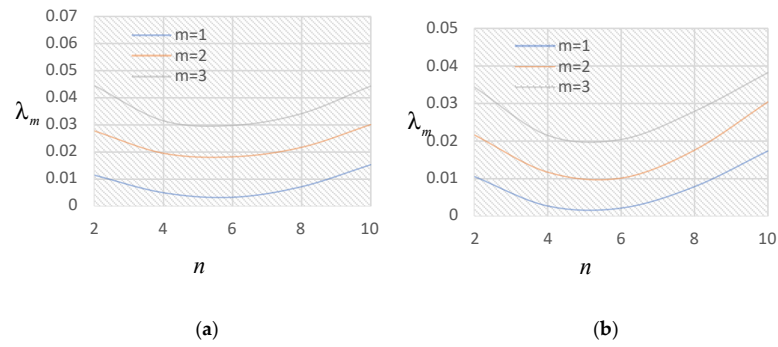
Figure 9. Effect of circumferential node number on the frequency parameter. (**a**) Five-layered ($0°/90°/0°/90°/0°$) Graphite Epoxy/Kevlar Epoxy/Graphite Epoxy/Kevlar Epoxy/Graphite Epoxy. (**b**) Six-layered ($0°/90°/0°/90°/0°/90°$) Graphite Epoxy/Kevlar Epoxy/Graphite Epoxy/Kevlar Epoxy/Graphite Epoxy/Kevlar Epoxy shells under the effect of exponential thickness variation.

(**a**) (**b**)
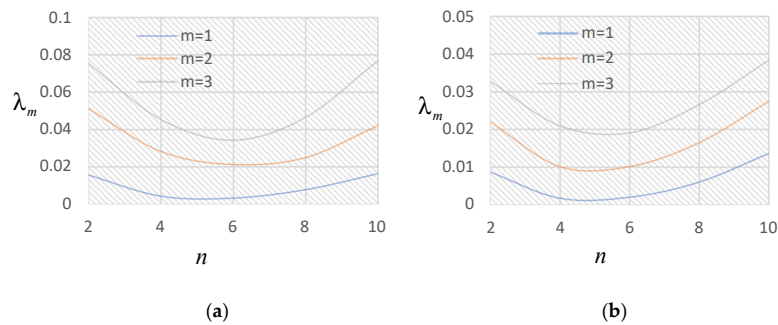
Figure 10. Effect of circumferential node number on the frequency parameter. (**a**) Five-layered ($0°/90°/0°/90°/0°$) Graphite Epoxy/Kevlar Epoxy/Graphite Epoxy/Kevlar Epoxy/GraphiteEpoxy. (**b**) Six-layered ($0°/90°/0°/90°/0°/90°$) Graphite Epoxy/Kevlar Epoxy/Graphite Epoxy/Kevlar Epoxy/Graphite Epoxy/Kevlar Epoxy shells under the effect of sinusoidal thickness variation.
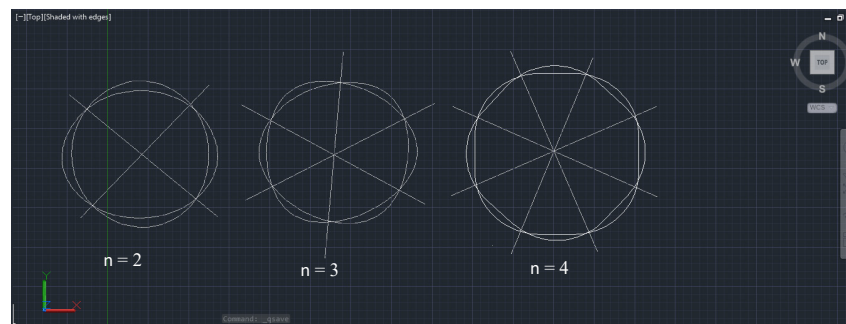
(**a**) Circumferential vibration forms (top view).
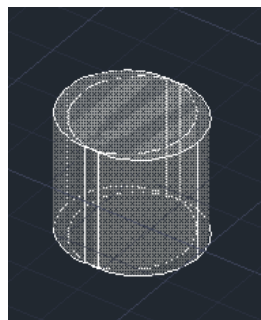
(**b**) Circumferential vibration forms.
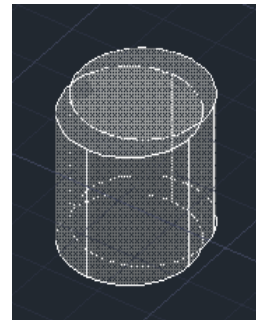
(**c**) Circumferential vibration forms (n = 2) (lateral view).

Figure 11. Circumferential vibration forms: (**a**) top view, (**b**,**c**) lateral view.

4. Conclusions

This study was based on the free vibration of conical shells of non-uniform thickness, consisting of two to six symmetric cross-ply layers, with each layer consisting of a different material under the influence of HSDT for simply supported end conditions. The main aim of this study was to investigate the vibration of shells and to achieve lower frequency values for more stable structures. In order to achieve this aim, shells of non-uniform thickness and consisting of different layers were considered. It is evident from the results that as the number of layers of conical shells increases, the frequency values decrease. Moreover, by varying length ratios and cone angles, shells with non-uniform thickness have lower frequency values compared to shells of constant thickness. So, the objective of achieving lower frequency values was fulfilled by non-uniform thickness and increasing the number of layers of the shells. In conclusion, the results evidently show the appropriateness of the methodology used.

Conflicts of Interest: The author declares that they have no conflicts of interest regarding the publication of this paper.

References

1. Maji, A.; Mahato, P.K. Development and applications of shear deformation theories for laminated composite plates: An overview. *J. Thermoplast. Compos. Mater.* **2022**, *35*, 2576–2619. [CrossRef]
2. Carrera, E.; Ciuffreda, A. A unified formulation to assess theories of multilayered plates for various bending problems. *Compos. Struct.* **2005**, *69*, 271–293. [CrossRef]
3. Li, D. Layerwise theories of laminated composite structures and their applications: A review. *Arch. Comput. Methods Eng.* **2021**, *28*, 577–600. [CrossRef]
4. Banijamali, S.M.; Jafari, A.A. Free vibration analysis of rotating functionally graded conical shells reinforced by anisogrid lattice structure. *Mech. Based Des. Struct. Mach.* **2023**, *51*, 1881–1903. [CrossRef]
5. Aris, H.; Ahmadi, H. Using the higher-order shear deformation theory to analyze the free vibration of stiffened rotating FGM conical shells in a thermal environment. *Thin-Walled Struct.* **2023**, *183*, 110366. [CrossRef]
6. Shadmani, M.; Afsari, A.; Jahedi, R.; Kazemzadeh-Parsi, M.J. Nonlinear free vibrations analysis of truncated conical shells made of bidirectional functionally graded materials. *J. Vib. Control* 2023. [CrossRef]
7. Wang, Z.Q.; Yang, S.W.; Hao, Y.X.; Zhang, W.; Ma, W.S.; Zhang, X.D. Modeling and free vibration analysis of variable stiffness system for sandwich conical shell structures with variable thickness. *Int. J. Struct. Stab. Dyn.* **2023**, *23*, 2350171. [CrossRef]
8. Cho, J.R. Free Vibration Responses of Functionally Graded CNT-Reinforced Composite Conical Shell Panels. *Polymers* **2023**, *15*, 1987. [CrossRef]
9. Hu, S.; Zhong, R.; Wang, Q.; Qin, B.; Shao, W. A strong-form Chebyshev-RPIM meshless solution for free vibration of conical shell panels with variable thickness and fiber curvature. *Compos. Struct.* **2022**, *296*, 115884. [CrossRef]
10. Peng, Q.; Wang, Q.; Chen, Z.; Zhong, R.; Liu, T.; Qin, B. Dynamic stiffness formulation for free vibration analysis of rotating cross-ply laminated combined elliptical-cylindrical-conical shell. *Ocean Eng.* **2023**, *269*, 113486. [CrossRef]
11. Chanda, A.; Sahoo, R. Trigonometric zigzag theory for free vibration and transient responses of cross-ply laminated composite plates. *Mech. Mater.* **2021**, *155*, 103732. [CrossRef]
12. Reddy, J.N. *Mechanics of Laminated Composite Plates and Shells: Theory and Analysis*; CRC Press: Boca Raton, FL, USA, 2004.
13. Singha, T.D.; Rout, M.; Bandyopadhyay, T.; Karmakar, A. Free vibration of rotating pretwisted FG-GRC sandwich conical shells in thermal environment using HSDT. *Compos. Struct.* **2021**, *257*, 113144. [CrossRef]
14. Deb Singha, T.; Bandyopadhyay, T.; Karmakar, A. Thermoelastic free vibration of rotating pretwisted sandwich conical shell panels with functionally graded carbon nanotube-reinforced composite face sheets using higher-order shear deformation theory. *Proc. Inst. Mech. Eng. Part L J. Mater. Des. Appl.* **2021**, *235*, 2227–2253. [CrossRef]
15. Gia Ninh, D.; Tri Minh, V.; Van Tuan, N.; Chi Hung, N.; Van Phong, D. Novel numerical approach for free vibration of nanocomposite joined conical–cylindrical–conical shells. *AIAA J.* **2021**, *59*, 366–378. [CrossRef]

16. Bagheri, H.; Kiani, Y.; Eslami, M.R. Free vibration of FGM conical–spherical shells. *Thin-Walled Struct.* **2021**, *160*, 107387. [CrossRef]
17. Safarpour, M.; Rahimi, A.R.; Alibeigloo, A. Static and free vibration analysis of graphene platelets reinforced composite truncated conical shell, cylindrical shell, and annular plate using theory of elasticity and DQM. *Mech. Based Des. Struct. Mach.* **2020**, *48*, 496–524. [CrossRef]
18. Afshari, H. Free vibration analysis of GNP-reinforced truncated conical shells with different boundary conditions. *Aust. J. Mech. Eng.* **2022**, *20*, 1363–1378. [CrossRef]
19. Amabili, M.; Balasubramanian, P. Nonlinear forced vibrations of laminated composite conical shells by using a refined shear deformation theory. *Compos. Struct.* **2020**, *249*, 112522. [CrossRef]
20. Zhang, G.; Xiao, C.; Rahimi, A.; Safarpour, M. Thermal and mechanical buckling and vibration analysis of FG-GPLRC annular plate using higher order shear deformation theory and generalized differential quadrature method. *Int. J. Appl. Mech.* **2020**, *12*, 2050019. [CrossRef]
21. Taati, E.; Fallah, F.; Ahmadian, M.T. Closed-form solution for free vibration of variable-thickness cylindrical shells rotating with a constant angular velocity. *Thin-Walled Struct.* **2021**, *166*, 108062. [CrossRef]
22. Zarei, M.; Rahimi, G.; Shahgholian-Ghahfarokhi, D. Investigation on the free vibration behavior of sandwich conical shells with reinforced cores. *J. Sandw. Struct. Mater.* **2021**, *24*, 900–927. [CrossRef]
23. Guo, S.; Hu, P.; Li, S. Free vibration analysis of composite conical shells using Walsh series method. *Mater. Res. Express* **2021**, *8*, 075303. [CrossRef]
24. Maji, P.; Singh, B.N. Shear deformation theory for free vibration responses of 3D braided pre-twisted conical shells under rotation. *Int. J. Comput. Methods Eng. Sci. Mech.* **2022**, *23*, 99–118. [CrossRef]
25. Pakravan, I.; Heidari Soureshjani, A.; Talebitooti, R.; Talebitooti, M. Haar wavelet technique applied on the functionally graded carbon nanotube reinforced conical shells to study free vibration and buckling behaviors in thermal environments. *J. Vib. Control* **2022**, *28*, 1863–1878. [CrossRef]
26. Wang, X.; Lin, H.; Zhu, Y.; Wu, W. Vibro-acoustic modelling of immersed cylindrical shells with variable thickness. *Int. J. Nav. Archit. Ocean Eng.* **2020**, *12*, 343–353. [CrossRef]
27. Thai, C.H.; Ferreira AJ, M.; Nguyen-Xuan, H.; Phung-Van, P. A size dependent meshfree model for functionally graded plates based on the nonlocal strain gradient theory. *Compos. Struct.* **2021**, *272*, 114169. [CrossRef]
28. Phung-Van, P.; Lieu, Q.X.; Ferreira AJ, M.; Thai, C.H. A refined nonlocal isogeometric model for multilayer functionally graded graphene platelet-reinforced composite nanoplates. *Thin-Walled Struct.* **2021**, *164*, 107862. [CrossRef]
29. Saira, J. Free vibration characteristic of laminated conical shells based on higher-order shear deformation theory. *Compos. Struct.* **2018**, *204*, 80–87.
30. Javed, S.; Viswanathan, K.K.; Aziz, Z.A.; Prabakar, K. Free vibration of anti-symmetric angle-ply plates with variable thickness. *Compos. Struct.* **2016**, *137*, 56–69. [CrossRef]
31. Spath, H. Interpolation by Certain Quantic Splines. *Comput. J.* **1969**, *12*, 292–293.
32. Schoenberg, I.J.; Whitney, A. On Polya Frequency Functions 111. The Positivity of Translation Determinants with an Application to the Interpolation Problem by Spline Curves. *Trans. Am. Math. Soc.* **1953**, *74*, 246–259.
33. Bickley, W.G. Piecewise Cubic Interpolation and Two-Point Boundary Problems. *Comput. J.* **1968**, *11*, 206–208. [CrossRef]
34. Irie, T.; Yamada, G.; Tanaka, K. Natural frequencies of truncated conical shells. *J. Sound Vib.* **1984**, *92*, 447–453. [CrossRef]
35. Liew, K.M.; Ng, T.Y.; Zhao, X. Free vibration analysis of conical shells via the element-free kp-Ritz method. *J. Sound Vib.* **2005**, *281*, 627–645. [CrossRef]
36. Dai, Q.; Cao, Q.; Chen, Y. Free vibration analysis of truncated circular conical shells with variable thickness using the Haar wavelet method. *J. Vibroeng.* **2016**, *18*, 5291–5305. [CrossRef]
37. Kumar, A.; Bhargava, P.; Chakrabarti, A. Vibration of laminated composite skew hyper shells using higher order theory. *Thin-Walled Struct.* **2013**, *63*, 82–90. [CrossRef]